



# Interference Source Location Based on Spaceborne Multi-beam Antenna

Cen Ruan<sup>1,2</sup>, Laiding Zhao<sup>1,2</sup>(✉), Gengxin Zhang<sup>1,2</sup>, and Jidong Xie<sup>1,2</sup>

<sup>1</sup> Key Laboratory of Broadband Wireless Communication and Sensor Network Technology, Nanjing University of Posts and Telecommunications, Nanjing 210003, China  
zhaold@njupt.edu.cn

<sup>2</sup> “Telecommunication and Network” National Engineering Research Center, Nanjing University of Posts and Telecommunications, Nanjing 210003, China

**Abstract.** Based on the frequency division multiplexing principle of the multi-beam antenna, this paper proposes a new method for locating interference sources by only one single satellite. According to the antenna pattern function expression of multi-beam antennas, the positioning equations are derived and established by analyzing the link that interfering signal arrives at the spaceborne multi-beam antenna from the ground. Importantly, the gain error is introduced in the positioning process when we evaluate the performance of this positioning method. Considering the difficulty of solving nonlinear positioning equations, a new algorithm combining the Particle Swarm Optimization (PSO) and grid search is proposed. At the same time, in this paper, in order to analyze the feasibility of this new algorithm, we introduce the Monte Carlo method in the process of this experiment. Finally, this new algorithm is compared with the traditional Particle Swarm Optimization in terms of speed and accuracy, which shows the superiority of this new algorithm.

**Keywords:** Interference source location · Single-satellite · Multi-beam antenna · Gain error · PSO combined with grid-search

## 1 Introduction

In the recent years, satellite communication has developed rapidly because of its outstanding coverage, wide communication distance, and no geographical restrictions. Nowadays, the application of satellites is not limited to communication, but is permeated in various fields such as navigation, positioning, military reconnaissance, and weather forecasting [1, 2]. For the satellites with large-scale multi-beam antennas, while their sensitivity of the received signal is improving, they are more susceptible to various intentional or unintentional interference, which affect the operation of the satellite systems to a great extent [3]. Therefore, it is extremely urgent to find a quick and effective method to locate the interference source.

Traditional technology for interference source location are based on time difference of arrival (TDOA), frequency difference of arrival (FDOA), and angle of arrival (AOA)

[4–7]. Although these methods have the superiority of high positioning accuracy, fast positioning speed, and low system complexity, however, at least two qualified satellites are required in these positioning systems. In order to avoid the difficulty of selecting qualified satellites and decrease the consumption of orbit resources, a positioning method based on single satellite is proposed. This positioning technology is proposed to positioning the interference source with three co-frequency beams of the multi-beam antenna, according to the frequency division multiplexing principle, which provides a new idea for locating interference sources. At the same time, in order to further improve the positioning accuracy and reduced positioning time, a particle swarm optimization algorithm combined on grid search is proposed in this paper. By introducing the meshing process for the PSO, the PSO can be significantly optimized in terms of positioning error and time complexity.

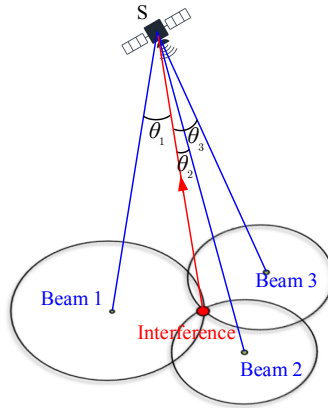


Fig. 1. Positioning model

## 2 Positioning Principle

Reference [8] gives the function expression of the multi-beam antenna pattern, which proposes that the antenna gain can be approximately calculated by the angle between the signal incident direction and the beam center pointing.

$$G = G_0 \left[ \frac{J_1(u)}{2u} + 36 \frac{J_3(u)}{u^3} \right]^2 \tag{1}$$

Where  $J_1$  and  $J_3$  are first-order and third-order Bessel function of first kind respectively,  $u = 2.07123 \sin\theta / \sin(\theta_{3dB})$ ,  $G_0 = \pi^2 D^2 \eta / \lambda^2$  is the beam center gain,  $\theta_{3dB}$  refers to half-power beam width,  $\theta$  refers to the angle between the incident direction of the interference signal and the center of the beam,  $D$  refers to antenna aperture,  $\eta$  refers to antenna efficiency, and  $\lambda$  refers to wavelength of the radiation signal.

For a spaceborne multi-beam antenna, its gain overlap between the co-frequency beam is large. And when the interference signal is strong, the main interfered beam

and the co-frequency multiplexed beams that are close to the interference source all can receive this interference signal [9, 10]. The location of the interference source can be acquired by the characteristics that different beams can receive different interference signal strengths. The positioning model is shown in Fig. 1.

### 2.1 Formula Derivation

In order to obtain the positioning equations, the link characteristics in the Fig. 1 are analyzed below.

It's assumed that the coordinate of the satellite, the coordinates of the center points of *beam 1*, *beam 2*, and *beam 3* are known. And they are expressed in terms of the vectors  $r_s, r_1, r_2$ , and  $r_3$  in the space rectangular coordinate system. The coordinates of interference source is represented as  $r_I = (x, y, z)$ . For *beam i* ( $i = 1,2,3$ ), the interference source, satellite, and *beam i* form a triangle. According to the cosine theorem, angle between the incident direction of the interference signal and the *beam i* center pointing can be expressed as

$$\theta_i = \arccos \frac{|r_s - r_i|^2 + |r_s - r_I|^2 - |r_I - r_i|^2}{2|r_s - r_i||r_s - r_I|} \tag{2}$$

Combining the antenna pattern function expression which is given by Eq. 1, the gains of the interference signals in *beam 1*, *beam 2*, and *beam 3* can be obtained as  $G(\theta_1), G(\theta_2)$ , and  $G(\theta_3)$ .  $G(\theta_1)$  means that when the incident angle of the radiation signal is  $\theta_1$ , the intensity of the radiation obtained by *beam 1* is  $G(\theta_1)$ .

When interfering signals reach the satellite from the ground, it is assumed that the transmission loss is denoted as  $L$ , the transmitting power of the interference source is  $P_t$ , and the satellite antenna gain is  $G_t$ . For *beam 1*, the interference signal strength received by *beam 1* is assumed to be  $P_1$ . And the link equation can be derived as following.

$$[P_1] = [P_t] + [G_t] + [G(\theta_1)] - [L] \tag{3}$$

The interference signal strengths acquired in *beam 2* and *beam 3* are assumed to be  $P_2$  and  $P_3$ . Then, the equal gain equations (unit: dB) can be listed as

$$\begin{cases} [P_1] = [P_t] + [G_t] + [G(\theta_1)] - [L] \\ [P_2] = [P_t] + [G_t] + [G(\theta_2)] - [L] \\ [P_3] = [P_t] + [G_t] + [G(\theta_3)] - [L] \end{cases} \tag{4}$$

By eliminating  $[P_t]$ ,  $[G_t]$ , and  $[L]$ , and combining the earth ellipsoid model equation in the WGS-84 coordinate system [11], we can get

$$\begin{cases} [P_2] - [P_1] = [G(\theta_2)] - [G(\theta_1)] \\ [P_3] - [P_2] = [G(\theta_3)] - [G(\theta_2)] \\ x^2 + y^2 + \frac{z^2}{1 - e^2} = a^2 \end{cases} \tag{5}$$

where  $a$  is semi-major axis of the earth ellipsoid mode and  $e$  is the first eccentricity of the earth ellipsoid mode under the WGS-84 coordinate system.

### 3 Error Analysis

#### 3.1 Theoretical Derivation

In the positioning process, the position of the interference source is given by Eq. 5. In this section, we will consider the gain error, beam center position error, and elevation error. Equation 5 can be transformed as

$$\begin{cases} \lambda_{21} = f_{21} \\ \lambda_{32} = f_{32} \\ x^2 + y^2 + \frac{z^2}{1 - e^2} = a^2 \end{cases} \tag{6}$$

Where  $\lambda_{21} = [P_2] - [P_1]$ ,  $\lambda_{32} = [P_3] - [P_2]$ ,  $f_{21} = [G(\theta_2)] - [G(\theta_1)]$ ,  $f_{32} = [G(\theta_3)] - [G(\theta_2)]$ .

We total differentiate Eq. 6 to get:

$$\begin{cases} d\lambda_{21} = \frac{\partial f_{21}}{\partial x} dx + \frac{\partial f_{21}}{\partial y} dy + \frac{\partial f_{21}}{\partial z} dz + \frac{\partial f_{21}}{\partial x_1} dx_1 + \frac{\partial f_{21}}{\partial y_1} dy_1 + \frac{\partial f_{21}}{\partial z_1} dz_1 + \frac{\partial f_{21}}{\partial x_2} dx_2 + \frac{\partial f_{21}}{\partial y_2} dy_2 + \frac{\partial f_{21}}{\partial z_2} dz_2 \\ d\lambda_{32} = \frac{\partial f_{32}}{\partial x} dx + \frac{\partial f_{32}}{\partial y} dy + \frac{\partial f_{32}}{\partial z} dz + \frac{\partial f_{32}}{\partial x_2} dx_2 + \frac{\partial f_{32}}{\partial y_2} dy_2 + \frac{\partial f_{32}}{\partial z_2} dz_2 + \frac{\partial f_{32}}{\partial x_3} dx_3 + \frac{\partial f_{32}}{\partial y_3} dy_3 + \frac{\partial f_{32}}{\partial z_3} dz_3 \\ da = \frac{x}{a} dx + \frac{y}{a} dy + \frac{z}{a(1 - e^2)} dz \end{cases} \tag{7}$$

Then transform Eq. 7 into a matrix form

$$dE = W_0 dX + W_1 dX_1 + W_2 dX_2 + W_3 dX_3 \tag{8}$$

The final positioning error of the interference source can be expressed as

$$dX = W_0^{-1} (dE - W_1 dX_1 - W_2 dX_2 - W_3 dX_3) \tag{9}$$

Where

$$\begin{aligned} W_0 &= \begin{bmatrix} \frac{\partial f_{21}}{\partial x} & \frac{\partial f_{21}}{\partial y} & \frac{\partial f_{21}}{\partial z} \\ \frac{\partial f_{32}}{\partial x} & \frac{\partial f_{32}}{\partial y} & \frac{\partial f_{32}}{\partial z} \\ \frac{x}{a} & \frac{y}{a} & \frac{z}{a(1 - e^2)} \end{bmatrix}, W_1 = \begin{bmatrix} \frac{\partial f_{21}}{\partial x} & \frac{\partial f_{21}}{\partial y} & \frac{\partial f_{21}}{\partial z} \\ 0 & 0 & 0 \\ 0 & 0 & 0 \end{bmatrix} \\ W_2 &= \begin{bmatrix} \frac{\partial f_{21}}{\partial x_2} & \frac{\partial f_{21}}{\partial y_2} & \frac{\partial f_{21}}{\partial z_2} \\ \frac{\partial f_{32}}{\partial x_2} & \frac{\partial f_{32}}{\partial y_2} & \frac{\partial f_{32}}{\partial z_2} \\ 0 & 0 & 0 \end{bmatrix}, W_3 = \begin{bmatrix} 0 & 0 & 0 \\ \frac{\partial f_{32}}{\partial x_3} & \frac{\partial f_{32}}{\partial y_3} & \frac{\partial f_{32}}{\partial z_3} \\ 0 & 0 & 0 \end{bmatrix} \\ dE &= \begin{bmatrix} d\lambda_{21} \\ d\lambda_{32} \\ da \end{bmatrix} \\ dX &= \begin{bmatrix} dx \\ dy \\ dz \end{bmatrix} \\ dX &= \begin{bmatrix} dx_i \\ dy_i \\ dz_i \end{bmatrix} \quad i = 1, 2, 3 \end{aligned}$$

### 3.2 Simulation Analysis

In order to discuss the performance of the positioning method proposed above, this section analyzes the influence of some errors on final positioning accuracy. In the simulation, it is assumed that the center position of *beam* 1, 2, and 3 are  $(E136.383^\circ, N39.9^\circ)$ ,  $(E124.067^\circ, N30.75^\circ)$ , and  $(E139.283^\circ, N26.083^\circ)$  respectively. The location of the satellite bottom point is  $(E113.383^\circ, N29.967^\circ)$ . The satellite orbital altitude is 35786km and orbital inclination is  $0^\circ$ .

When the interference source is in different positions, we will discuss the influence of the gain measurement error on the positioning accuracy. Considering the gain measurement error with 1 dB ( $d\lambda_1 = d\lambda_2 = 1$  dB), and the results are shown in Fig. 2.

In Fig. 2, it can be seen that when the interference source is close to the center of a certain beam, the positioning error is small. However, when the interference source is close to the center of the area surrounded by these three beams, the positioning error becomes large. Actually, the gain error has a great impact on the final positioning accuracy. When the gain error is 1 dB, the final location will be 10, 000 to 50, 000 m away from the real interference source.

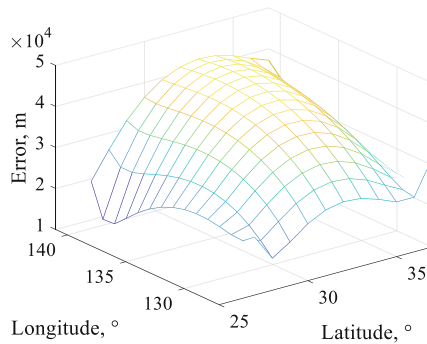


Fig. 2. Gain error

## 4 Algorithm

### 4.1 Particle Swarm Optimization Based on Grid Search

Considering that  $G(\theta_1)$ ,  $G(\theta_2)$ , and  $G(\theta_3)$  are non-linear functions, Eq. 5 belongs to a non-linear equation group. For nonlinear equations, Taylor expansion method and Newton iteration method are commonly used, but the solution process is mostly tedious [12, 13]. In order to further improve the positioning accuracy and reduced positioning time, a particle swarm optimization algorithm combined on grid search is proposed. Compared with the traditional particle swarm algorithm [14, 15], this algorithm mainly replaces the search task of some populations by dividing the grid and randomly taking points in these grids. For Eq. 5, the algorithm is described as follows.

1. establish an objective function  $f(x, y, z)$ :

$$f(x, y, z) = \text{sqrt}([(P_2 - P_1) - (G(\theta_2) - G(\theta_1))]^2 + [(P_3 - P_2) - (G(\theta_3) - G(\theta_2))]^2) \quad (10)$$

2. Initialization

Unknown components  $x$  and  $y$  are randomly generated in the three beam centers, and this is used as the initial position of the population in the particle swarm search. The optimal solution searched by particle swarm algorithm in two-dimensional space is denoted as  $(x_0, y_0)$ .

3. With  $(x_0, y_0)$  as the center point, create a square search area  $S$  near  $(x_0, y_0)$ . In the area  $S$ , the grid is continuously refined by repeatedly taking points randomly to find the point closest to the true location of the interference source. The specific method is as follows:

- Step1: Divide the square search area into four sub-grids in a grid
- Step2: Randomly take multiple random points  $(x,y)$  in these four sub-grids. The component  $z$  is solved by the model equation of the earth ellipsoid  $x^2 + y^2 + \frac{z^2}{1-e^2} = a^2$
- Step3: Substitute  $(x,y,z)$  into the objective function for analysis and judgment, taking the random point with the smallest objective function value as the “local optimal solution” of this division.
- Step4: Divide the sub-grid where the point with the “local optimal solution” is located into four smaller sub-grids. Repeat steps 2 and 3 to continuously update the “local optimal solution” to determine which sub-mesh will be divided next time. After a certain number of times of grid division, the program is stopped, and the current “local optimal solution” is regarded as the global optimal solution of the interference source.

## 4.2 Algorithm Simulation

In this simulation, we assume that the center of beam 1, beam 2, and beam 3 are  $(E116.383^\circ, N39.9^\circ)$ ,  $(E104.067^\circ, N30.75^\circ)$ , and  $(E119.283^\circ, N26.083^\circ)$  respectively. It is assumed that the location of the satellite bottom point is  $(E113.383^\circ, N29.967^\circ)$ , the actual location of the interference source is  $(E113^\circ, N29^\circ)$ , the satellite orbital altitude is 35786 km and orbital inclination is  $0^\circ$ .

Considering the gain error has a great impact on the positioning accuracy, the gain error with 1 dB is introduced in the process of solving the equations. Based on Monte Carlo Method [15], a hundred simulations were performed, and the simulation results are shown in Fig. 3 and Fig. 4. The Fig. 3 shows the result of 10 iterations and Fig. 4 shows the result of 200 iterations.

The red five-pointed star in these two figures indicates the actual position of the interference source, and these blue points are the optimal solution found in each simulation. With the number of iterations increasing, these blue points become more and more concentrated near the true location of the interference source. The positioning errors of Fig. 3 and Fig. 4 are 36.724 km and 30.115 km respectively.

In order to prove the superiority of this algorithm, it is compared with the traditional particle swarm optimization algorithm.

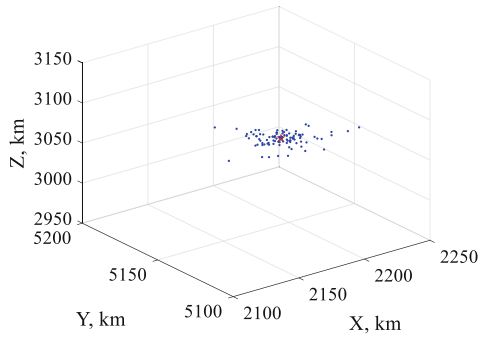


**Fig. 3.** 10 iterations of the positioning result

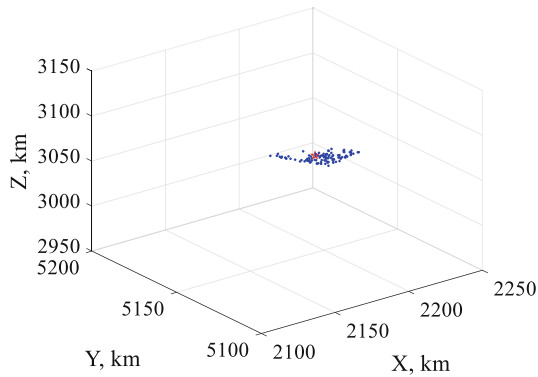


**Fig. 4.** 100 iterations of the positioning result

When using the traditional particle swarm algorithm to solve the positioning equations, we set the maximum number of iterations to 200 and the population size to 20. However, when using the improved algorithm to solve it, we reduced the population size to 10. For the grid-search part of the new algorithm, the grid is divided five times, and ten points are randomly selected from each sub-grid.

The simulation results are shown in the Fig. 5 and Fig. 6. Figure 5 shows the relationship between iteration times and positioning errors. Figure 6 shows the relationship between iteration times and positioning time. In these two pictures, the red solid line represents the traditional particle swarm optimization algorithm and the blue dotted line represents the improved algorithm.

Taking the simulation parameters of this paper as an example, the convergence speed of the two algorithms is basically the same, and they can basically achieve convergence when iterating 12 times.

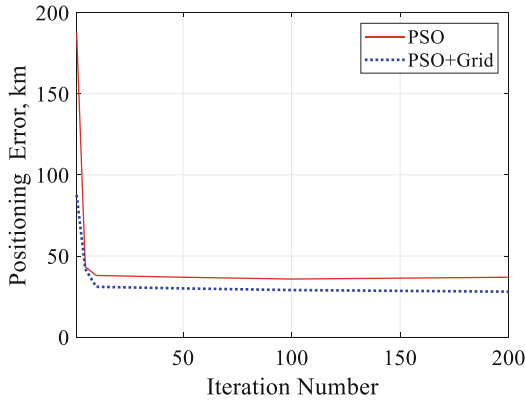


**Fig. 5.** Comparison of positioning accuracy

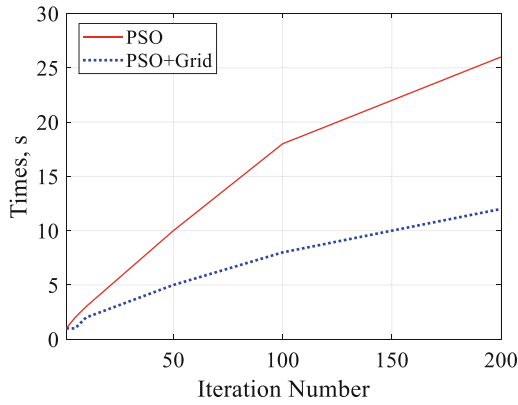


**Fig. 6.** Comparison of positioning time

In terms of time complexity: the improved algorithm reduces the number of initial populations in the PSO while introducing the process of meshing. By selecting the appropriate number of populations and the number of grid divisions, the speed of the algorithm can be effectively improved.

In terms of solving errors: the improved algorithm meshes within the error range after the convergence of the traditional particle swarm optimization algorithm to meet the requirements of higher positioning accuracy.

Meanwhile, Table 1 shows the positioning errors and positioning time of these two algorithms in 200 iterations.

The results show that both algorithms have strong convergence. After 200 iterations, the positioning time of the improved algorithm is reduced to half that of the traditional particle swarm optimization, and the positioning accuracy of the new algorithm is also improved.

**Table 1.** Algorithm comparison

	Positioning accuracy (unit: meter)	Positioning time (unit: second)
PSO	3.67e + 04	27
PSO combined with meshing	3.01e + 04	14

## 5 Conclusion

Single-satellite positioning technology based on the spaceborne multi-beam antenna requires only one satellite, but its positioning accuracy is greatly affected by the gain measurement error. Then we introduce the gain measurement error when we solve the nonlinear positioning equations. Meanwhile, a particle swarm algorithm based on grid search is proposed to assist this experiment. In order to demonstrate the reliability of this new algorithm, we compare it with the traditional particle swarm algorithm in terms of speed and the accuracy, which shows the superiority of this new algorithm.

## References

1. Song, X., Ping, X.: Features of current foreign satellite communication systems and their developing trend. *Commun. Audio Video* (2014)
2. Mao-Qiang, Y., Dao-Xing, G., Lu, L.U.: *wireless communication technology*, 91, 1031–1041 (2012)
3. Vatalaro, F., et al.: Analysis of LEO, MEO, and GEO global mobile satellite systems in the presence of interference and fading. *IEEE J. Sel. Areas Commun.* **13**(2), 291–300 (1995)
4. Liu, C., Yang, J., Wang, F.: Joint TDOA and AOA location algorithm. *J. Syst. Eng. Electron.* **24**(2), 183–188 (2013)
5. Lin, X., You, H.E., Shi, P.: Location algorithm and error analysis for earth object using TDOA FDOA by dual-satellite and aided height information. *Chin. J. Space Sci.* **26**(4), 277–281 (2006)
6. Zhu, W.Q., et al.: Analysis of precision of multi-satellite joint location based on TDOA/FDOA. *Syst. Eng. Electron.* **31**(12), 2797–2800 (2009)
7. Wu, R., et al.: A novel long-time accumulation method for double-satellite TDOA/FDOA interference localization. *Radio Sci.* **53**(1), 129–142 (2018)
8. Caini, C., et al.: A spectrum- and power-efficient EHF mobile satellite system to be integrated with terrestrial cellular systems. *IEEE J. Sel. Areas Commun.* **10**(8), 1315–1325 (1992)
9. Sohyeun, Y., et al.: Multibeam reflector antenna for ka-band communication satellite. In: *Antennas & Propagation Society International Symposium. IEEE* (2012)
10. Matsumoto, Y., et al.: Satellite interference location system using on-board multibeam antenna. *Electron. Commun. Japan (Part I: Commun.)* **80**(11), 22–33 (2015)
11. Yu, Z.Y.: A location method based on WGS-84 earth model using satellites TDOA measurements. *J. Astronaut.* **24**(6) 569–573 (2003)
12. Julier, S., Uhlmann, J., Durrant-Whyte, H.F.: A new method for the nonlinear transformation of means and covariances in filters and estimators. *IEEE Trans. Autom. Control* **45**(3), 477–482 (2000)

13. Yan, G.: A newton method for a nonsmooth nonlinear complementarity problem. *Oper. Res. Trans.* **15**(15), 53–58 (2011)
14. Van den Bergh, F., Engelbrecht, A.P.: A study of particle swarm optimization particle trajectories. *Inf. Sci.* **176**(8), 937–971 (2006)
15. Liu, B., et al.: Improved particle swarm optimization combined with chaos. *Chaos Solitons & Fractals* **25**(5), 1261–1271 (2005)
16. Yeh, W.C., et al.: A particle swarm optimization approach based on monte carlo simulation for solving the complex network reliability problem. *IEEE Trans. Reliab.* **59**(1), 212–221 (2010)